PROCEEDINGS OF SPIE

SPIEDigitalLibrary.org/conference-proceedings-of-spie

Water adsorption beyond monolayer coverage on ZnO surfaces and nanoclusters

David Raymand, Tomas Edvinsson, Daniel Spångberg, Adri van Duin, Kersti Hermansson

David Raymand, Tomas Edvinsson, Daniel Spångberg, Adri van Duin, Kersti Hermansson, "Water adsorption beyond monolayer coverage on ZnO surfaces and nanoclusters," Proc. SPIE 7044, Solar Hydrogen and Nanotechnology III, 70440E (9 September 2008); doi: 10.1117/12.795337

SPIE.

Event: Solar Energy + Applications, 2008, San Diego, California, United States

Water adsorption beyond monolayer coverage on ZnO surfaces and nanoclusters

David Raymand[a], Tomas Edvinsson[a], Daniel Spångberg[a], Adri van Duin[b] and Kersti Hermansson[a]
[a]*Materials Chemistry, The Ångström Laboratory, Uppsala University, Box 538, S-75121 Uppsala, Sweden*
[b] *Material and Process Simulation Center, California Institute of Technology, Pasadena CA 91125, USA*

ABSTRACT

The surface structures of ZnO surfaces and ZnO nanoparticles, with and without water, were studied with a ReaxFF reactive force field (FF) and molecular dynamics (MD) simulations. The force field parameters were fitted to a training set of data points (energies, geometries, charges) derived from quantum-mechanical DFT/B3LYP calculations. The ReaxFF model predicts structures and reactions paths at a fraction of the computational cost of the quantum-mechanical calculations and as such allows dynamical simulations of reactive process for large (>>1000 atoms) and long (> 100 ps) timescales. Our simulations give the following results for the $(10\bar{1}0)$ surface. (i) The alternating H-bond pattern of Meyer et al. for a single monolayer coverage is reproduced by our simulations. This pattern is maintained at elevated temperatures (600K). (ii) At coverages beyond one water monolayer we observe enhanced ZnO hydroxylation at the expense of ZnO hydration. (iii) This is achieved through an entirely new H-bond pattern mediated via the water molecules in the second layer above the ZnO surface. (iv) During a water desorption simulation at T=300K we observe that the desorption rate slows significantly when two monolayers remain. (v) Simulations of nanoparticles in the presence and absence of water suggest that water plays a key role in the determination of nanoparticle shape by catalyzing surface reconstruction reactions and stabilizing specific surface structures.

Keywords: W*ater adsorption, zinc oxide, hydroxylation, hydrogen bonding, molecular dynamics simulation*.

1. INTRODUCTION

Zinc oxide (ZnO) is a wide bandgap semiconductor with a broad range of applications, owing to its diverse physical properties and the advanced and finely-tuned preparation processes available for ZnO materials. It has found a broad range of applications, including uses as a pigment and protective coating and as a UV absorbing additive in everything from skin cream to advanced plastic and rubber composites and applications in opto- and thermoelectronics. The ZnO properties can be changed and, in some aspects, fine-tuned with different dopants and synthesis methods, leading to present day applications that span the vast field of nano-electronics. For example, ZnO has been used in photocopy machines, transparent conducting layers, varistors, as optical wave guides, surface acoustic wave transducers, LEDs, laser diods, thin film transistors, and solar cells [1-3]. Moreover, ZnO has found applications in the field of heterogeneous catalysis, as it is able to catalyze a number of chemical reactions, including methanol formation from CO/H_2 and H_2 formation from the water gas shift reaction [4,5].

Solar Hydrogen and Nanotechnology III, edited by Gunnar Westin,
Proc. of SPIE Vol. 7044, 70440E, (2008) · 0277-786X/08/$18 · doi: 10.1117/12.795337

Zinc oxide in its normal crystalline form has a hexagonal wurtzite-type structure, with a surface morphology dominated by four faces: $(10\bar{1}0)$, $(11\bar{2}0)$, (0001) and $(000\bar{1})$ [11]. The optical band gap of wurtzite ZnO is 3.3 eV [6] at room temperature and show excitonic behavior. The high exciton binding energy of ZnO, 60 meV, gives a higher resistance for thermally induced exciton recombination compared to other semiconductors. For comparison, the thermal energy is 26 meV at room temperature and the exciton binding energies of e.g. ZnSe and GaN are 22 meV and 25 meV, respectively. This makes ZnO a promising candidate for room temperature exciton lasers in UV or near UV.

ZnO is also frequently used in nanoparticle applications. For example, ZnO nanoparticles have been integrated in mesoporous metal oxide electrodes, consisting of interconnected nanoparticles, which have been vital in the development of devices for catalysis, gas sensing, and solar cells [1,3]. The nanoparticles enhance the surface area per unit volume in the device and significantly improve the kinetics and mass transfer at the interfaces of the electrodes. In going towards nanoparticles, a large fraction of the material's atoms are surface atoms and a full understanding of the surface processes isparamount to elucidate the mechanisms. In the catalytic and gas sensing processes, the importance of the surface area enhancement is self-evident. In addition, the electronic and catalytic properties depend on the surface/volume ratio of the particle. If the size of the ZnO nanostructure e.g. is smaller than the Bohr radii of ZnO at ~ 6 nm [3], the material has been found to display quantum-confinement effects such as increased band gap. This can be conceived by orbital repulsion from not fully developed band structures but has also been seen to depend on the surface and its adsorbed species. In fact also in larger particles, the surface region displays modified electrical properties while keeping the physical properties within the bulk. For example, the conduction band (CB) edge positions of ZnO, TiO2 and other metal oxide semiconductors (MOSs) are known to have a Nernstian shift of +59 meV per pH unit [7,8] in aqueous solution caused by the change in surface -H+ and -OH− groups. Li+ is also known to adsorb at the TiO2 surface, giving it a positive charge that shifts ECB to more positive potentials. Due to the affinity to ZnO and TiO2, the small Li+ ion is, in the same way as H+, a potential determining ion, shifting the band edge to more positive potentials by adsorption on the ZnO or TiO2 surface. Dipole molecules, with the negative part towards the MOS surface, contribute to a negative surface charge, thus leaving ECB at a more negative potential. This is utilized in the so called nanostructured dye-sensitized solar cell (nDSSC) [9], where the addition of a dipolar molecule give a dramatic increase in efficiencies due to higher photovoltages [10]. CB edge tuning by surface adsorption is nowadays used in all high efficiency nDSSCs.

In summary, the ZnO surface properties play an immense role for the technological applications as well as for the fundamental understanding of electrical properties at the surface and the catalytic activity of ZnO. In order to fully access the more complicated processes at the surfaces it is necessary to begin with the metal oxide surface itself and, in particular, to study the hydroxylation/hydration process with water.

Water is present in many of the processes taking place at ZnO surfaces, including reactions catalyzed by ZnO, as an intermediate product, a side product or a product. One obvious case where water makes a difference is the methanol synthesis reaction from syngas (H_2,CO,CO_2), where the reverse water-gas shift reaction always has to be considered. ZnO-based catalysts are used in commercial synthesis of methanol. [5]

In this contribution we discuss theoretical calculations of water interactions with ZnO surfaces, extended systems and nanoparticles. Two fundamental goals are to understand whether the water adsorption is reversible or irreversible, and whether water is adsorbed molecularly or dissociatively. Determining whether the adsorption is irreversible is a relatively easy task from an experimental standpoint, as irreversible adsorption is usually accompanied by evolution of gases or a permanent alteration of the surface composition. For example water dissociation is the mechanism behind the oxidation of many materials. Identifying if water is adsorbed molecularly or dissociatively is difficult with experimental techniques. The difficulties lie in the similarity of H_2O and OH in many of their spectroscopic properties. Determining whether the adsorption is molecularor dissociative is important, since the dissociation products (OH, H and O) are chemically very different from water.[12]

Recently, a set of combined experimental and theoretical studies of the water adsorption on ZnO were published by Meyer and co-workers [13-15]. Using quantum-mechanical (DFT) calculations the experimentally found surface

structure for monolyarer coverage of water on the ZnO($10\bar{1}0$) could be verified. It was thus shown both in experiment and theory that a monolayer of water on the ZnO($10\bar{1}0$) consists of alternating molecularly adsorbed water and dissociated water, forming an ordered (2×1)-pattern. This structure is described as a “key-lock". The phenomenon was explained by the fact that within the monolayer every other water donates a hydrogen bond (“key") to the neighboring water molecule (“lock") thus activating it for dissociation, i.e. the reaction is self-catalyzed. ZnO($10\bar{1}0$) acts as a template ordering the water molecules into a favorable configuration [15]. Cooke et al. [16] also studied a monolayer of water on ZnO, by means of DFT calculations and static atomistic calculations with the Born model; their results supported the findings of Meyer et al. Apart from these studies, the theoretical literature concerning the atomic-level structure of water/ZnO interfaces is quite scare. The experimental literature of the water/ZnO system is more abundant and we refer to Ref. [5] for a comprehensive review.

In the current study we aim to go beyond monolayer coverage and also study water/ZnO interfaces at elevated temperature for relatively long simulation times. Quantum mechanical model systems are often limited to less than a hundred atoms and short simulation times if dynamics is invoked. Such systems are too small to describe the complex structure of nanoparticles, for example. To perform studies on large, water solvated nanoparticles (>>1000 atoms) we have developed a reactive force field (FF) within the ReaxFF framework [17], for use in molecular dynamics (MD) simulations addressing the reaction dynamics for ZnO. The force field parameters were fitted to a training set of data points (energies, geometries, charges) derived from quantum-mechanical (QM) B3LYP calculations. The force field model is able to predict structures and reactions paths with a similar level of quality as the data in the training set at a fraction of the computational cost of the QM-calculations.

Here we discuss the ZnO surface behavior with respect to hydration/hydroxylation with this ReaxFF Zn/O/H description. To validate the force field approach we first present results for the same system as studied by Meyer et al. [15] and Cooke et al. [16] and we present how temperature affects the resulting structures. Thereafter, we present results for larger water coverages, as well as for nanosystems. This is a first step into a deeper understanding of the surface properties of ZnO in aqueous solution.

2. METHOD

The most stable polymorph of Zinc oxide at ambient conditions is the wurtzite type structure (space group $P6_3mc$; No. 186 in *the International Tables for X-ray Crystallography*) with lattice constants a = 3.24992(5) Å and c = 5.20658(8) Å [18]. The MD simulations in this work were performed with a recently developed Zn/O/H potential within the ReaxFF force field framework. A brief account of the ReaxFF methodology and force field refinement is given in the following section.

2.1 The ReaxFF methodology

The ReaxFF system energy for the Zn/O/H system is divided into several components (Eq (1)). These energy components are a subsection of the general ReaxFF description (e.g. Chenoweth et al.[19]) and as such can be fully integrated with other ReaxFF descriptions.

$$E_{system} = E_{bond} + E_{over} + E_{under} + E_{lp} + E_{val} + E_{vdWaals} + E_{Coulomb} \quad (1)$$

These partial contributions comprise bond energies (E_{bond}), contributions penalizing overcoordination and (optionally) stabilizing undercoordination of atoms (E_{over} and E_{under}), lone-pair energies (E_{lp}), valence angle energies (E_{val}) and terms to handle non-bonded interactions, namely van der Waals ($E_{vdWaals}$) and Coulomb ($E_{Coulomb}$) interactions. All terms except the last two are bond-order dependent and as such are dependent on the local environment of each atom. A detailed description of the individual terms can be found in Refs. [17, 19, 20].

2.2 The force field optimization

The ReaxFF for ZnO was optimized using a successive one-parameter search technique as described by van Duin et al. [21]. The parameterization procedure used here consisted of the following steps:

(i) Create a training set from B3LYP calculations for clusters, crystals and crystal surfaces (energies, geometries, charges).
(ii) Fit the ReaxFF parameters to the data set.
(iii) Validate the potential parameters by comparing properties extracted from the model to experimental and quantum chemical data from other studies.

The current force field model is based on the ZnO parameters from ref [22]. The force field was extended to include the interaction with water by including the water parameters from ref [23]. To ensure the quality of this extension, additional data points were added to the training set, and the ZnO parameters were reparameterized to improve the fit (resulting in a small change of the original parameters). The original ZnO training set mainly comprised data from different condensed phases of ZnO. However, it also included three Zn(s) polymorphs and Zn-OH gas-phase clusters. Structures far from equilibrium were included since features of these might be important for the morphology of nanoparticles, where the small shape may induce a high concentration of grain boundaries and irregular surfaces; see **Fig 1**.

To train the new model's ability to describe the interaction between water and ZnO, a number of data points describing water dissociation profiles and adsorption geometries on the Wurtzite($10\bar{1}0$) surface were included since the ($10\bar{1}0$) face is the most studied and understood surface. Among other data points, nine adsorption geometries and two dissociation profiles published by Meyer et al. [5] were included (after the geometries had been reoptimized with B3LYP), [24]. A more detailed analysis of our water-ZnO force-field will be published elsewhere [24].

.

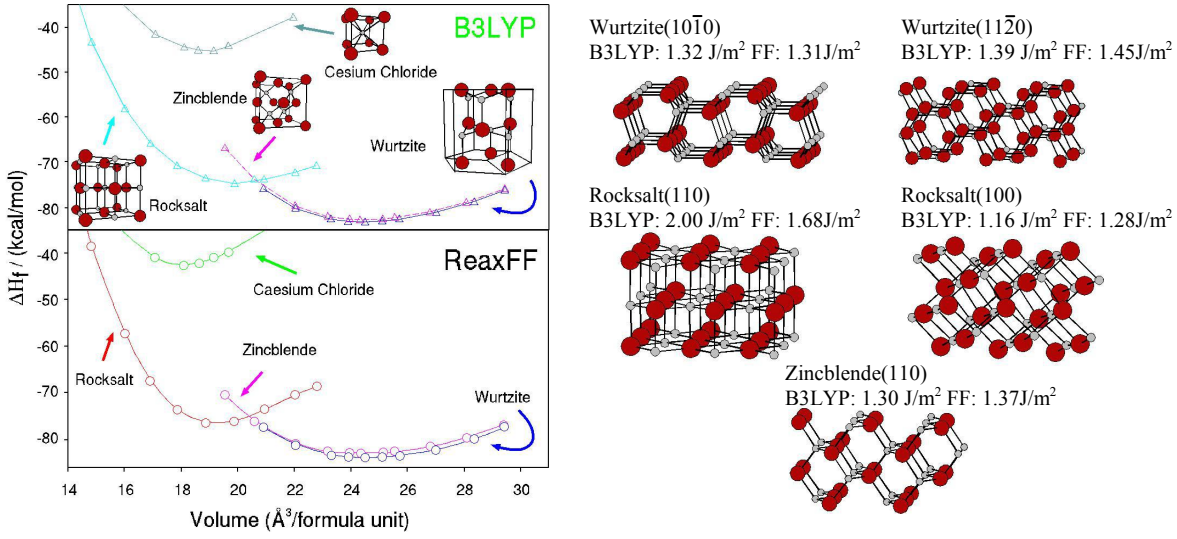

(a) **(b)**

Fig 1. Comparison of our ReaxFF model with the reference B3LYP calculations. a) Equation of state (compression and expansion) for four crystal structures of ZnO (wurtzite, zincblende, caesium chloride and rocksalt), b) Surface energies for five non-polar ZnO faces. Here and in the following figures oxygen is red, zinc is grey and hydrogen is white.

2.3 Molecular dynamics simulations

Short-time and small-scale simulations (< 1000 particles, < 200 ps) were performed with the built-in molecular dynamics routine of the ReaxFF software package [25] because of its good equilibration capabilities. Longer production simulations of bigger systems were performed with the GRASP software package [26] because of its parallel implementation. In all simulations, the equations of motion were solved with the velocity-verlet algorithm [27], using a time-step of 0.25 fs for the ZnO/water interface simulations and 0.50 fs for the ZnO simulations (without water).

In all simulations of surface systems, a 12-layer $Zn_{288}O_{288}$-slab with $\{10\bar{1}0\}$ surfaces on opposite sides was used under 3-D periodic boundary conditions.

In the *monolayer simulations*, each of the opposite slab surfaces was covered with 24 water molecules (corresponding to one water molecule per surface Zn). The slabs were separated by a vacuum gap of 75 Å, making them essentially non-interacting (quasi 2D-periodic). The simulations ran for 100 ps at three temperatures (10 K, 300 K and 600 K) in the constant volume, constant temperature ensemble (NVT), using the Berendsen thermostat [28] and the ReaxFF software package. The initial structures were geometry optimized using a molecular mechanics optimizer before the MD simulations started.

For *high water coverage* (a "liquid water" film), the model consisted of the same $Zn_{288}O_{288}$-slab, but the vacuum gap was replaced by a ~20 Å region filled with 256 water molecules (~20 Å thick layer). Here, the simulations were performed in the constant pressure, constant temperature ensemble (NPT) using the Nose-Hoover barostat and thermostat [29] and the GRASP software package. The temperature and pressure were set to 300 K and 1 atm, respectively. Prior to the 250 ps production simulations, the system was equilibrated for 250 ps.

The final structure of the 300K "liquid water" simulation was used as starting geometry for simulation of *water evaporation* from the ZnO surface. However, first a ~150 Å vacuum gap was introduced in the middle of the 20 Å thick water region. This resulted in a ZnO slab with each of its two opposite surfaces covered by 10 Å of water (128 water molecules corresponding to 5.3 times the monolayer coverage). At regular intervals, any desorbed water molecule (separated more than 10 Å from the adsorbed film) was removed from the MD box. The simulation was performed in the NVT ensemble using Nose-Hoover thermostat and the GRASP software package.

We also simulated *ZnO nanoparticles*, under three different conditions: immersed in water, monolayer coverage and vacuum. Three different nanoparticles were created in the same way, by cutting out a ZnO particle from the bulk structure. The particles was terminated with the low-energy $\{10\bar{1}0\}$ surfaces, the polar zinc terminated (0001) and oxygen terminated $(000\bar{1})$ surfaces.

The model system of a *nanoparticle immersed in water* consisted of a $Zn_{48}O_{48}$ particle (1 nm diameter) and 437 water molecules (in total 1407 atoms). The simulation time was 250 ps and the temperature was set to 300 K and the pressure to 1 atm. The simulations were performed under 3D-periodic boundary conditions in the NPT ensemble (Nose-Hoover thermostat and barostat) using the GRASP software package.

In the simulations of a *nanoparticle in vacuum* or *a nanoparticle covered with a monolayer of water*, 3D-periodic boundary conditions were used, but the particle was separated from its periodic images with 60 Å of vacuum, making them non-interacting (quasi-nonperiodic). The particles were allowed to reconstruct and relax by annealing at 1500 K in the NVT ensemble (Nose-Hoover thermostat) using the GRASP software package. The initial structures were geometry optimized using the molecular mechanics optimizer in the ReaxFF software package.

The model for a nanoparticle covered with 1 ML water was a $Zn_{420}O_{420}$ particle (2 nm diameter) and 168 water molecules (in total 1344 atoms). The simulation time was 250 ps. For the simulations of a nanoparticle in vacuum conditions was a $Zn_{825}O_{825}$ particle. The simulation time was 2.5 ns.

3. RESULTS

The results section is divided into three parts. Section 3.1 discusses simulations of ZnO slabs exposed to monolayer coverage of water, i.e. one H_2O (dissociated or not) per surface ZnO. Section 3.2 discusses ZnO slabs immersed in liquid water. In section 3.3 we present results from simulations of ZnO nanoparticles under three different conditions: immersed in liquid water, monolayer coverage and vacuum, and we discuss similarities with the extended surfaces.

3.1 Water monolayer on the ZnO($10\bar{1}0$) surface

Our simulations of the water/ZnO($10\bar{1}0$) at 300K system agree with the predictions of Meyer et al [15], refered to in the introduction. Thus, the (2x1)-pattern found in Ref. [15] remains even as the temperature is increased in our simulations. This can be seen in the middle panel of **Fig. 2**. It is also seen from **Fig. 2** that the same equilibrium structure is found independently of the adsorption geometry at the start – molecular or hydroxylated. **Fig. 3** shows how the H_2O and OH coverages vary as a function of time: the equilibrium structure is seen to be reached quickly, in only 20 ps.

The reason for the H-bonded zig-zag pattern being so stable is that the energy gain from the hydrogen bonding in a fully molecularly adsorbed monolayer is similar to the energy loss due to the non-optimal adsorption structure. In the case of fully dissociative adsorption, the energy gain from the dissociation does not compensate for the energy loss in hydrogen bonding. In the mixed molecular and dissociative adsorption pattern the dissociated water is stabilized by hydrogen bond donation from the non-dissociated water molecule [30].

At a temperature of 600 K we find a similar structure, which is formed after tens of picoseconds of simulation independent of the starting structures (**Fig. 2**). Moreover, when the water coverage lowers due to evaporation, the hydroxylation/hydration ratio remains constant. Indeed, **Fig. 3** shows in a more quantitative way that, at equilibrium, a 1:1 water-hydroxyl ratio is maintained on the ZnO($10\bar{1}0$) surface, even as water molecules evaporates at higher temperatures and the coverage drops. At 10 K, the system is unable to move out of the initial configuration.

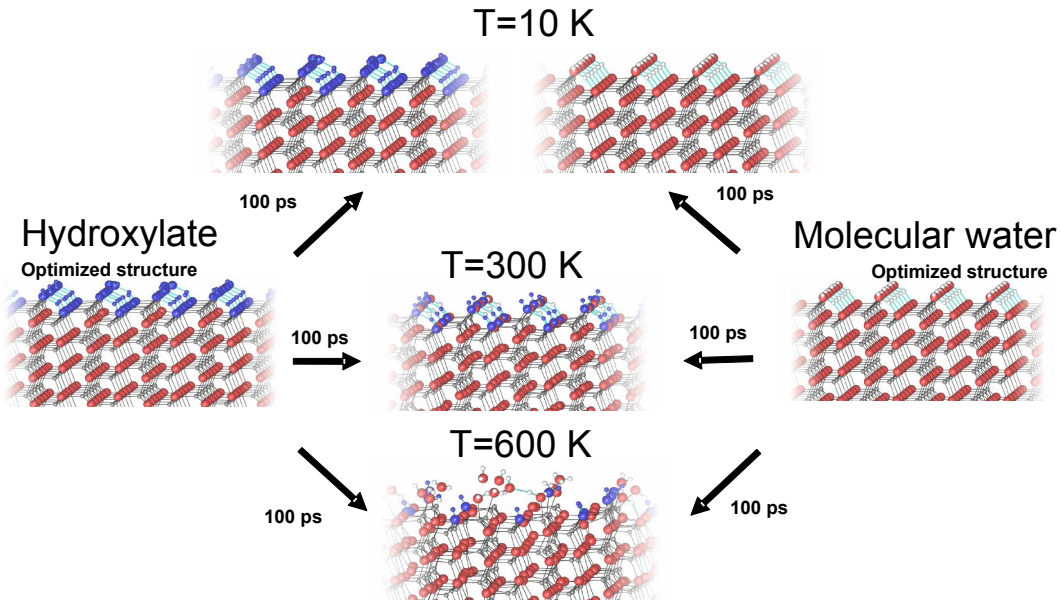

Fig 2. MD simulation of a monolayer of water on the ZnO($10\bar{1}0$) surface. The model system is a 12-layer $Zn_{288}O_{288}$ slab covered with 24 water molecules on each of the opposite sides. The simulations ran for 100 ps at three temperatures. Two different starting adsorption structures were used: Molecular water and dissociated water (i.e. a fully hydroxylated surface). The same equilibrium structure is reached at 300 K and 600 K regardless of whether the starting structure is dissociatively or molecularly adsorbed water molecules. The dissociated water, i.e. hydroxyl groups, have been colored blue.

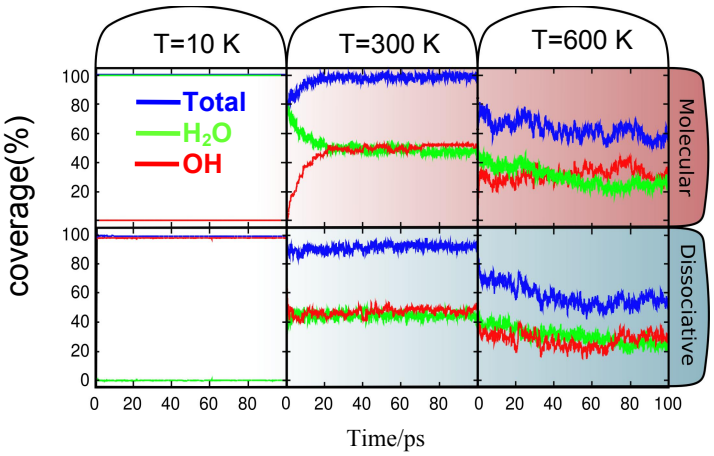

Fig 3. Time variation of the coverage of the surface adsorbates during the simulations in **Fig.2**, starting from a fully molecular water system and a fully dissociated system The color scheme for the graph is: OH(red), H_2O(green), total (blue).

3.2 ZnO surfaces immersed in water

This section describes our simulation results using water coverages extending beyond one monolayer. Here a layered structure with alternating water and ZnO layers was used as a model, as described in the Method section. The system was simulated for 250 ps at 300 K (**Fig. 4a**). To analyse the barrier for the reaction governing the hydroxylation/hydration ratio, the potential of mean force was calculated by taking the negative logarithm of O-H pair distribution function for water molecules and hydroxyls bound to the ZnO surface. We find that the system has indeed reached equilibrium, since the low barrier (5kT) indicates a fast and dynamic equilibrium between molecular and dissociated water (**Fig. 4b**).

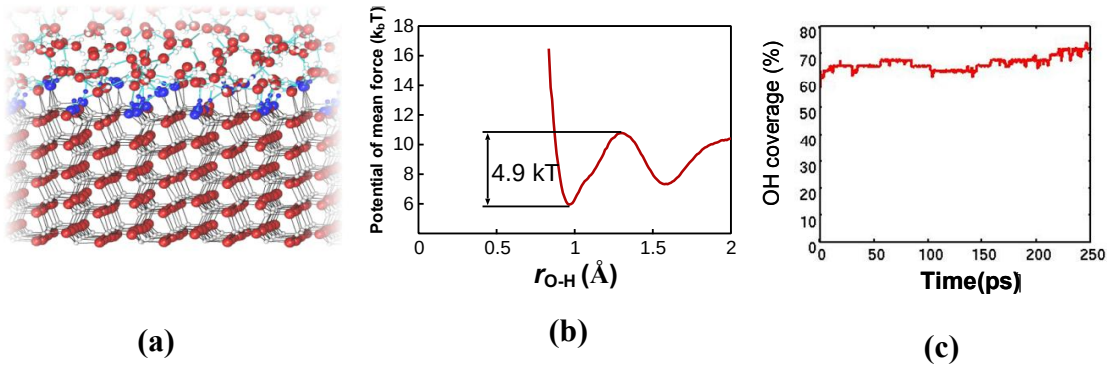

Fig 4 MD simulation of a model liquid water/ZnO interface at 300K. The model system is a 12-layer $Zn_{288}O_{288}$-slab with a region of 256 water molecules. The dissociated water molecules, i.e. the hydroxyl groups, have been colored blue. a) Snapshot at the end of the MD simulation, b) Potential of mean force obtained from the simulation. c) OH coverage in %.

An analysis of the water/ZnO interface shows that, compared to the monolayer simulations, the equilibrium coverage of the surface is pushed towards hydroxylation. The reason for this is the increased possibility of hydrogen bonding with the water phase outside the first monolayer. In fact, an entirely new H-bond situation is created, where practically all water molecules in the first layer dissociate, leaving OH groups which donate and accept hydrogen bonds from the water molecules in the second layer above the ZnO surface. These water molecules thus function as mediators of H-bonding between the surface -OH groups. A close-up of the interface structure from **Fig 4a** is seen in **Fig. 5a** (see section 2.3 for details).

To test if this increased hydroxylation and the new H-bond pattern remain when the water content decreases we started from the configuration depicted in **Fig. 4a** and ran a simulation where water molecules were allowed to evaporate at 300 K and leave the system (see Method section). During this simulation we find two separate desorption regimes as a function of time (**Fig 6)**. When the coverage drops below two water molecules per surface Zn (corresponding to twice the coverage of a monolayer), the rate of desorption drops significantly. An analysis of the structure in **Fig. 5b** shows that for this coverage, the hydroxylation/hydration pattern is quite similar to that of the ZnO/liquid interface in **Fig. 5a**, only slightly distorted, because now there is no H-bond network from the liquid keeping the OH groups and water in place.

These results are in agreement with hypotheses based on experimental observations by Nagao[31], Hirschwald et al [32]. and Zwicker et. al [33], who, based on IR-measurements and thermal desorption measurements, suggested that the ZnO the metal oxide surface is hydroxylated with molecular water adsorbed onto these hydroxyls.

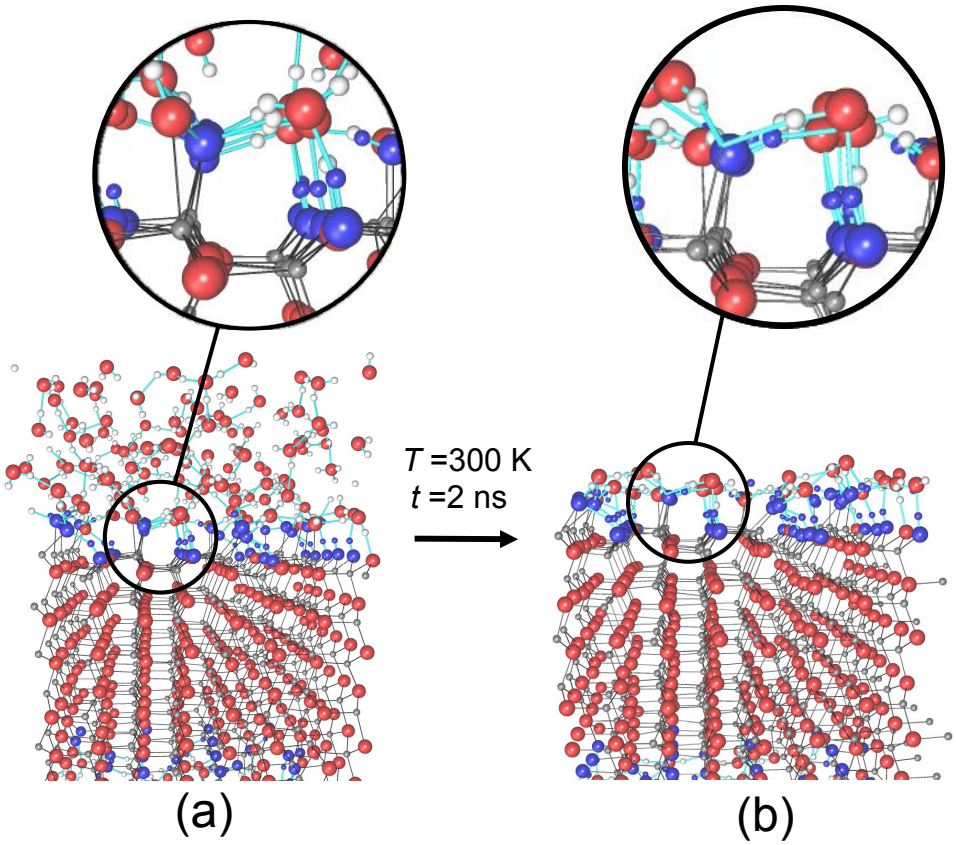

Fig 5. MD simulation of a $Zn_{288}O_{288}$-slab with 12 ZnO layers and initially 256 water molecules at 300 K, starting from the end of the simulation in **Fig 4a**. The hydroxyl groups have been colored blue. (a) MD snapshot before evaporation, (b) MD snapshot after evaporation.

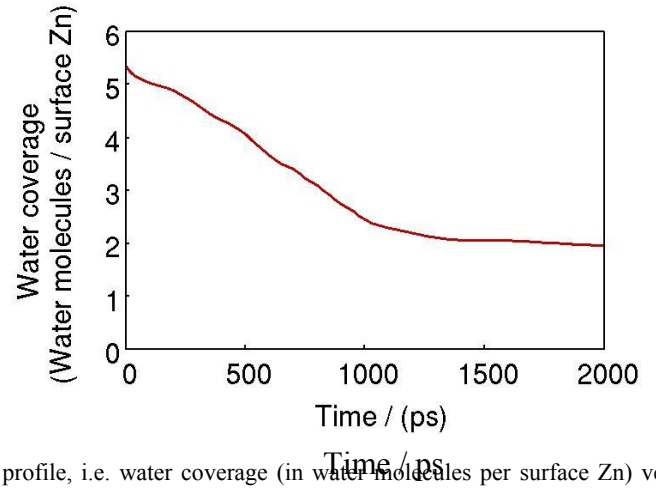

Fig 6. Desorption profile, i.e. water coverage (in water molecules per surface Zn) versus simulation time at 300 K for the process shown in **Fig. 5**. One water molecule per surface Zn corresponds to monolayer coverage.

3.3 ZnO nanoparticles

3.3.1 A 1 nm nanoparticle immersed in liquid water

Our simulations of a 1 nm nanoparticle immersed in liquid water give rise to a similar degree of hydroxylation as for the extended ZnO surface immersed in water (**Fig 7**). Therefore we can assume that the nanoparticle has a similar effect on water dissociation as found in section 3.2 for the extended surface (i.e. a low barrier). The low dissociation barrier is connected with an increased proton-transfer rate between surface hydroxyls/adsorbed waters. When a water dissociates on the non-polar $(10\bar{1}0)$-surface the surface Zn ions accepts the OH group while the surface O ions accept the extra proton, forming two hydroxyl-groups. For the nanoparticle we also see hydroxylation of the polar Zn-teminated (0001) and O terminated $(000\bar{1})$ surface. Our hypothesis is that the excess proton from a water molecule dissociated on the Zn-terminated surface is transferred to the O-terminated surface through a *"Grotthuss"* like effect, facilitated by the increased proton-transfer rate at the ZnO surface. We aim to validate this hypothesis in the future using longer-timescale simulations, which will allow for more rigorous statistical evaluation..

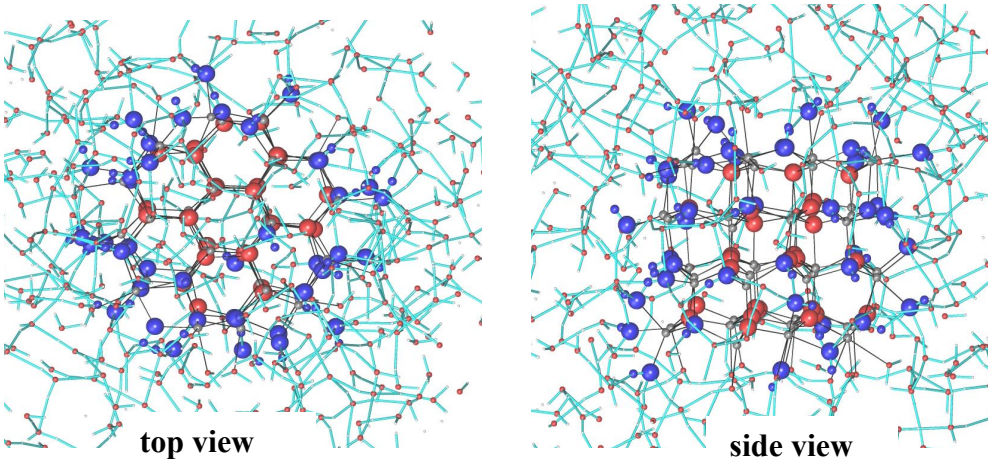

Fig 7. Snapshot from an MD simulation (NPT) of a 1 nm large $Zn_{48}O_{48}$ nanoparticle immersed in 437 water molecules at 300 K after 250 ps, starting from an ideal bulk cluster. Here and in **Fig. 8** and **Fig 9**, the nanoparticle has the wurtzite structure, and is terminated by $(10\bar{1}0)$ surfaces on the sides, and (0001) and $(000\bar{1})$ on the top and bottom, respectively. Hydroxyls are blue. The nanoparticle is seen from two directions (top view and side view).

3.3.2 Nanoparticles annealed at 1500K with and without water

To investigate the influence of water on nanoparticle reconstruction we performed high-temperature (1500K) simulations on the nanoparticle in the presence and absence of water. The annealed clean nanoparticle in **Fig. 8** and the hydrated (1 ML) nanoparticle in **Fig. 9** clearly both undergo reconstruction at 1500 K. The particles have become more spherical, to decrease their total surface areas. The effect of the water layer has been to "catalyze" the reconstruction. Already at a tenth of the simulation time the particle initially covered with water has undergone larger reconstruction than the vacuum nanoparticle. Close inspection of the hydroxylation reveals that step sites (where the atomic layers with the (0001) as normal are broken) are chiefly hydroxylated, thus stabilizing them.

This allows the reconstruction towards a more spherical particle to pass through configurations with a high concentration of these high energy step sites. In the vacuum case, the particle has to pass through a more disordered surface layer to achieve the reconstruction. The dipole-moment of the particle may be the driving force behind the reconstruction with access to water the particle can more easily counteract its dipole moment, without resorting to disordered regions. We aim to study these mechanism in more detail in the future using longer-timescale simulations.

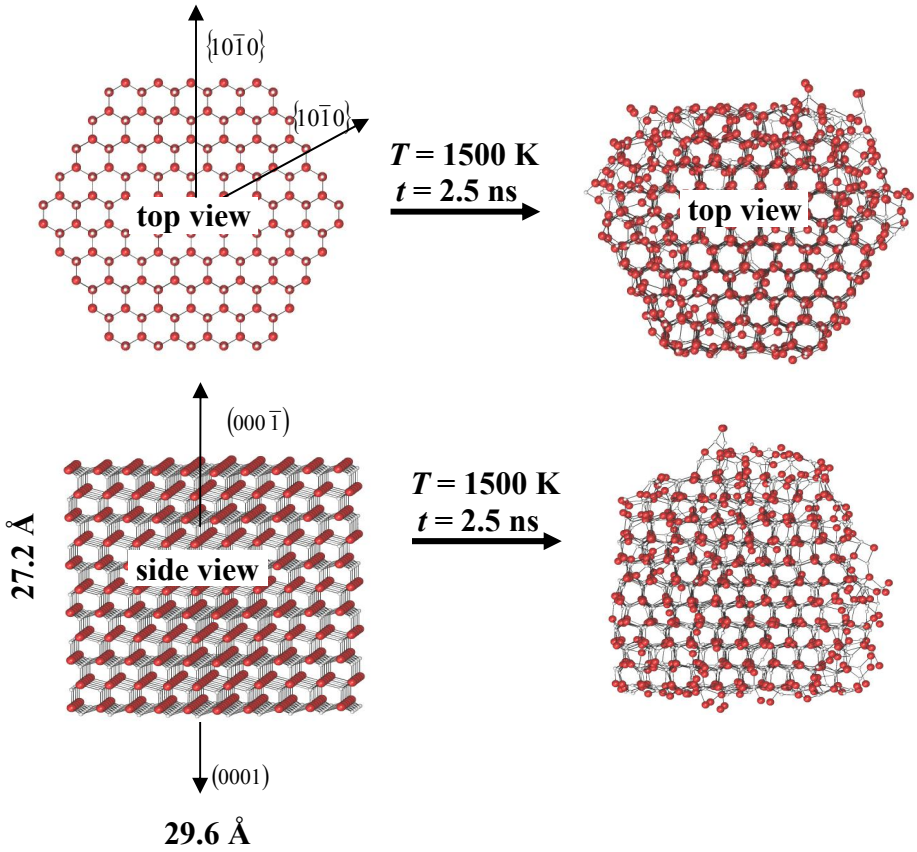

Fig 8. 3nm $Zn_{825}O_{825}$ nanoparticle, initially in the wurtzite structure, before and after annealing at 1500K using an MD simulations in the NVT ensemble.

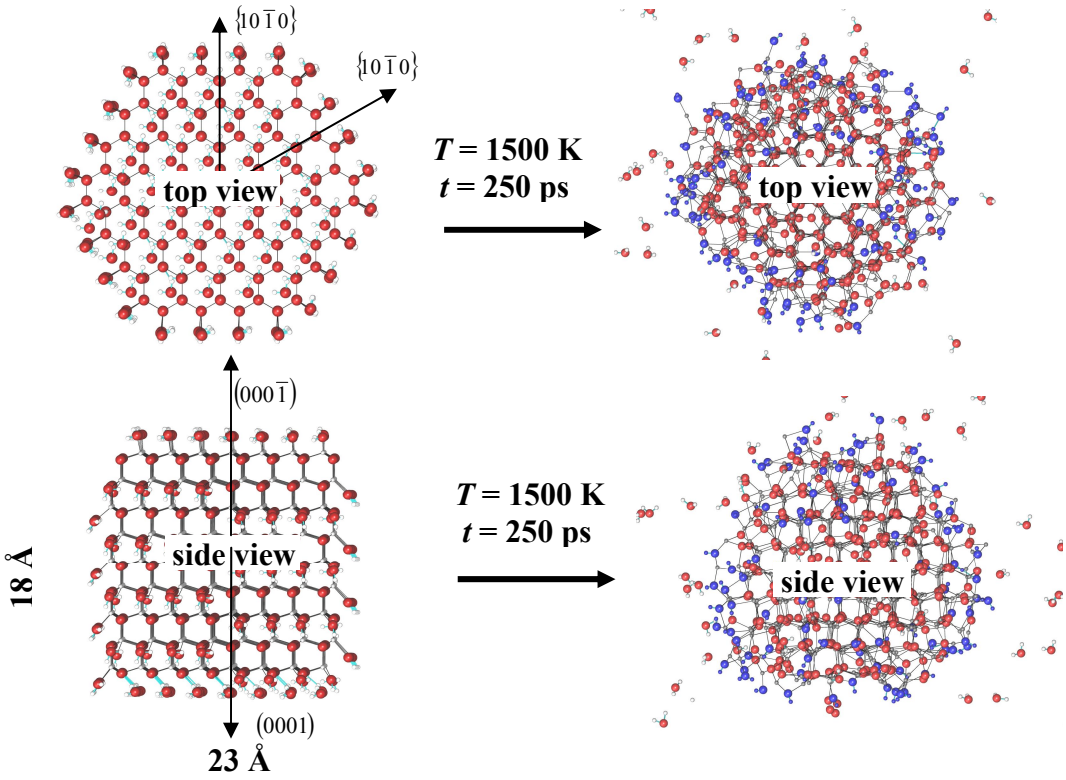

Fig 9. 2nm $Zn_{420}O_{420}$ nanoparticle, initially in the wurtzite structure, and 168 water molecules before and after annealing at 1500K using an MD simulations in the NVT ensemble.

4. CONCLUSIONS

We have performed molecular dynamics simulations on ZnO-surfaces and nanoparticles in the presence and absence of water using a ReaxFF reactive force field for Zn/O/H interactions. Our force field approach was validated by means of repeating the simulations performed in an earlier QM-based study [15], which predicted a (2x1)-pattern adsorption pattern of water on the ZnO($10\bar{1}0$) surface, resulting in a 50% hydroxyl-covered surface. Our force field reproduced these patterns and predicted that this pattern remains even as the temperature is increased. Moreover, we find that when the coverage increases beyond a monolayer, the equilibrium coverage of the surface is pushed towards higher hydroxylation levels, reaching a hydroxylation level of up to 70%. The reason for this is that the additional water layers provide an increased possibility of hydrogen bonding with the water phase outside the first monolayer.

We performed a water desorption simulation at T=300K. Here we observed two separate desorption regimes. When the coverage drops below two water molecules per surface Zn (corresponding to twice the coverage of a monolayer), the rate of desorption drops, indicating that the water molecules here are bound more strongly.

In addition, we also performed high-temperature (1500K) simulations on $Zn_{420}O_{420}$ nanoparticles in the presence and absence of water. We find here that water effectively catalyzes surface reconstruction reactions, facilitating the transfer of the nanoparticle into a more energetically favorable shape.

The main conclusion of this work is that the interaction between water and ZnO affects the structure and properties of both the water layer as well as the ZnO surface structure. The specific new structures which form at the interface may very well have important mechanistic consequences for the many applications of zinc oxides..

Acknowledgement. This work has been supported by the Swedish Research Council (VR). Computer time was provided by the Swedish National Infrastructure for Computing (SNIC). The computations were performed at UPPMAX under Project s00707-54. This work was also supported by NSF ITR-grant DMR-0427177.

REFERENCES

[1] U. Ozgur, Y. I. Alivov, C. Liu, A. Teke, M. A. Reshchikov, S. Dogan, V. Avrutin, S. J. Cho, and H. Morkoc, J. Appl. Phys. **98** 041301 (2005).

[2] A. Tsukazaki, A. Ohtomo, T. Onuma, M. Ohtani, T. Makino, M. Sumiya, K. Ohtani, S. F. Chichibu, S. Fuke, Y. Segawa, H. Ohno, H. Koinuma, and M. Kawasaki, Nature Mater. **4** 42-46 (2005).

[3] G. Boschloo, T. Edvinsson, A. Hagfeldt, Dye-sensitized nanostructured ZnO Electrodes for solar cell applications. In *Nanostructured Materials for Solar Energy Conversion*; Soga, T., Ed.; Elsevier: Amsterdam 227-254 (2007).

[4] G. A. Somorjai, *Introduction to Surface Chemistry and Catalysis*, John Wiley & Sons Inc, New York, USA (1994).

[5] C. Wöll, Progress in Surface Science **82** 55120 (2007).

[6] S. A. Studenikin, N. Golego, and M. Cocivera, J. Appl. Phys. **84** 9 (1998).

[7] H. Gerischer, In *Photoelectrochemistry, Photocatalysis and Photoreactors*; M. Schiavello, Ed.; D. Reidel: Dordrecht, Germany, 39-106 (1985).

[8] A. J. Nozik, R. Memming, J. Phys. Chem. **100** 13061-13078 (1996).

[9] B. O'Regan, M. Grätzel, Nature. **353** 737-740 (1991).

[10] M. K. Nazeeruddin, A. Kay, I. Rodicio, R. Humphry-Baker, E. Muller, P. Liska, N. Vlachopoulos and M. Gratzel, J. Am. Chem. Soc. **115** 6382–6390 (1993).

[11] V. Henrich, A. Cox, *The Surface Science of Metal Oxides*; Cambridge University Press: Cambridge, UK (1994).

[12] M. Henderson, Surface Science Reports **46** 1-308 (2002).

[13] B Meyer, D. Marx, O. Dulub, U. Diebold, M. Kunat, D. Langenberg, C Wöll, Angew. Chem. Int. Ed. **43** 6642 (2004).

[14] O. Dulub, B. Meyer, U. Diebold, Phys.Rev. Lett. **95** 136101 (2005).

[15] B. Meyer, H. Rabaa, D. Marx, Phys. Chem. Chem. Phys. **8** 1513-1520 (2006).

[16] D.J. Cooke, A. Marmier, S.C. Parker, J. Phys Chem B, **110** 7985-7991 (2006)

[17] A.C.T. van Duin, S. Dasgupta, F. Lorant, W.A. Goddard III, J. Phys. Chem. A **105** 9396 (2001).

[18] J. Albertsson, S.C. Abrahams, Å. Kvick, Acta Cryst. B **45** 34 (1989).

[19] K. Chenoweth, A. C. T. van Duin, W.A. Goddard III J. Phys. Chem. A **112** 1040 (2008)

[20] A.C.T. van Duin, A. Strachan, S. Stewman, Q. Zhang, X. Xu, W.A. Goddard III, J. Phys. Chem. A **107** 3803 (2003).

[21] A.C.T. van Duin, J.M.A. Baas, B.J. van de Graaf, J. Chem. Soc. Faraday Trans. **90** 2881 (1994).

[22] D. Raymand, M. Baudin, A.C.T van Duin, K. Hermansson, Surf. Sci. **602** 1020-1031 (2008).

[23] A.C.T. van Duin, V. Bryantsev and W.A. Goddard, manuscript in preparation.

[24] D Raymand, D Spångberg, A.C.T van Duin, K, Hermansson, manuscript in preparation.

[25] A.C.T van Duin, California Institute of Technology , ReaxFF Reactive force field program.

[26] A.P. Thompson, Sandia National Laboratories, GRASP version 4.0.

[27] W. C. Swope,. C. Andersen, P. H. Berens, K. R. Wilson, J. Chem. Phys. **76** 637 (1982).

[28] H.J.C. Berendsen, J.P.M. Postma, W.F.V. Gunsteren, A. DiNola, J.R. Haak, J. Chem. Phys. **81** 3684 (1984).

[29] M. Tuckerman, B.J. Berne, G.J. Martyna, J. Chem. Phys. **97** 1990 (1992).

[30] M. Odelius, Phys. Rev. Lett. **82** 3919 (1999).

[31] M. Nagao, J.Chem. Phys. **75** 25 (1971).

[32] W. Hirschwald, *Zinc Oxide*, in: *Current topics in Materials Science* **7** 148 (1981).

[33] G. Zwicker, K. Jacobi, Surf. Sci. **131** 179 (1983).